ESRF	**Experiment title:** In situ SAXS/USAXS investigation of homogeneous and heterogeneous nucleation in a nanoparticle jet produced by Rapid Expansion of Supercritical Fluids	**Experiment number**: ME1177
Beamline: ID02	**Date of experiment**: from: 02.12.2005 to: 05.12.2005	**Date of report**:
Shifts: 9	**Local contact(s)**: Dr. Pierre Panine	*Received at ESRF:*

Names and affiliations of applicants (* indicates experimentalists):

Dipl.-Ing. Robert LINDNER*, ESA-ESTEC (NL)

Dipl.-Ing. Martin Steurenthaler*, ITTK, Universität Karlsruhe (D)

Prof. Dr.-Ing. Michael TUERK, ITTK, Universität Karlsruhe (D)

Preliminary Experiment Report ME1177

Introduction

In December 2005 we carried out experiments for the in situ interrogation of particle formation in a RESS jet. At the ESRF beamline ID02, nine shifts of beamtime were granted from 02.-05.12.2005 for proposal ME1177. Aim of this measurement campaign was to determine the radial and axial particle evolution in the RESS process jet [1,2,3]. A previous measurement campaign [4] showed the feasibility of resolving particle sizes in such a dilute system.

Experimental setup

A schematic representation of the setup is shown in Figure 1.

CO_2 is pumped from a solvent reservoir bottle (60 bar) (1) with a diaphragm metering pump (3) via a heat exchanger (2) (set at 5°C, to ensure that CO2 remains liquid), a buffer volume(3a) and the radiation lock (baffle, 4) into the thermostatic extraction unit (high-pressure cell (5), V=500ml, with extractor insert (6)) and hence pressurised up to 20MPa. This part of the setup is placed inside the hutch whereas the CO_2 bottle, the heat exchanger, the pump and the buffer is located outside the hutch.

The supercritical solvent is loaded with the solute in the thermostatic extraction unit. A burst disk (7) is installed for security reasons. It opens, if the pressure in the extractor/high pressure vessel exceeds 25MPa. The pressure cylinder and adjacent components are designed for pressures up to 35MPa. Thereafter, either pure CO_2 flows through the bypass section of the extraction unit or through the extractor (6) and then the capillary nozzle (50µm(10)). Gas and particles are collected via a hose and filter mounted above the nozzle.

Experiment Procedure

The extractor (6) is filled with a mixture of the substance to be micronized and glass beads. It is then inserted into the pressure vessel (5). The extractor/high pressure vessel is assembled again and all connectors are checked for tightness. This step however has to take place only every few experiment runs, since the extractor contains several grams of substance allowing for some hours of experiment time.

The pump is switched on and the pump speed regulated until a pressure of about 20MPa is reached in the pressure vessel (5). While the pump is running, the bypass section is opened enabling a steady flow of pure CO_2 through the nozzle (10). The temperature of the pressure vessel is set to the desired value. When all parameters (p,T) have reached the set value, the valve (8) is slowly opened while valve (9) is closed at the same time. CO_2 flows now through the extractor, loaded with the substances to be investigated. When the whole setup is working at constant parameters, the hutch will be closed and the beam shutters opened.

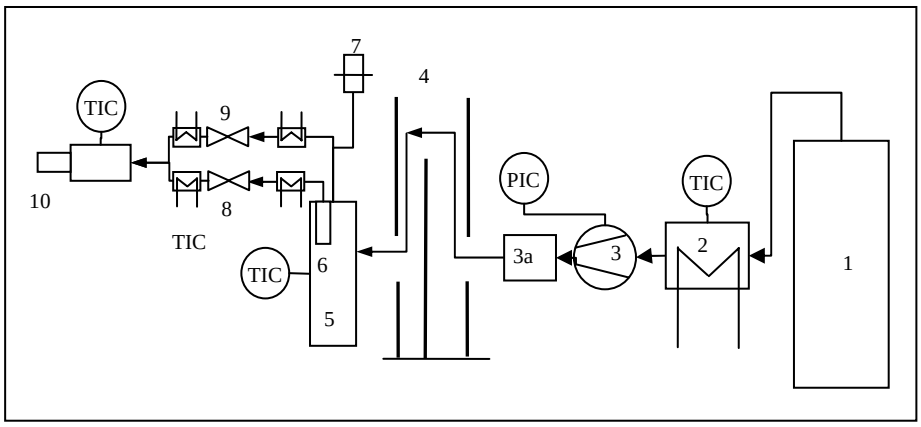

Figure 1 *The mobile RESS setup*

Figure 2 shows the nozzle front end mounted on the positioning stage in the experiment hutch. Radial and axial scans of the jet were performed with three different solutes (Phytosterol, benzoic acid, $Cu(TMHD)_2$) and as well with pure CO_2, using the pinhole setup of the high brilliance beamline ID02. The alignement of the nozzle with respect to the x-ray beam is checked before every new experiment and after every manipulation or maintenance at the nozzle front end. Background measurements were performed before the

jet is switched on, or in some cases, just after the experiment runs. Once the jet is running, all vertical and horizontal scans are performed, Experiments with salycic acid were aborted due to problems with the dust collection and venting. Table 1 summarises the experiment conditions during this campaign.
Compared to our first measurements in 2004, we did not encounter the total clogging of the nozzle. This was mainly due to our improved experiment setup, providing stable flow conditions in the jet. From the experiment results however it can be seen, that a partial clogging can occur and causes a slight asymmetry of the jet. The reason for this is most likely an instationarity in the nozzle temperature or the temperature of the heated ducting connecting the extractor with the nozzle, leading to a premature condensation of the solute.

Figure 2 *The heated nozzle mounted on the positionig table in front of the SAXS pinhole camera setup. The red line indicates the position of the x-ray beam, the blue line the position of the jet from a 50 µm nozzle.*

Table 1 *Experiment conditions for all experiment runs. Measurements with salycic acid were aborted due to problems with the dust collection*

Solvent/ solute	CO_2	CO_2/ Benzoic acid	CO_2/ Phytosterol	CO_2/ $Cu(TMHD)_2$	CO_2/Salycic acid
Temperature Extractor	48-50	48-50	48-50	48-50	48-50
Temperature range Nozzle [C]	67	75-85	66-70	70-72	67
Extraction pressure range[MPa]	19.5-20	19.5-20	19.5-20	19.5-20	19.5-20
Scan radial [mm]	-2 to 2	-2 to 2	-2 to 2	-2 to 2	-
Scan axial [mm]	0.3-10.3	0.3-9.8	0.3-9.8	0.3-9.8	-

Results

For the measurement evaluation, the antimasked background intensity scattering curves (no jet) were subtracted from those with jet. The averaged background intensity scattering curve during radial scans was steady, as shown in Figure 3. The dependence from the radial position can be neglected. Hence one averaged background intensity curve was used for all radial measurement in one plane. The integration time for each measurement was one second.

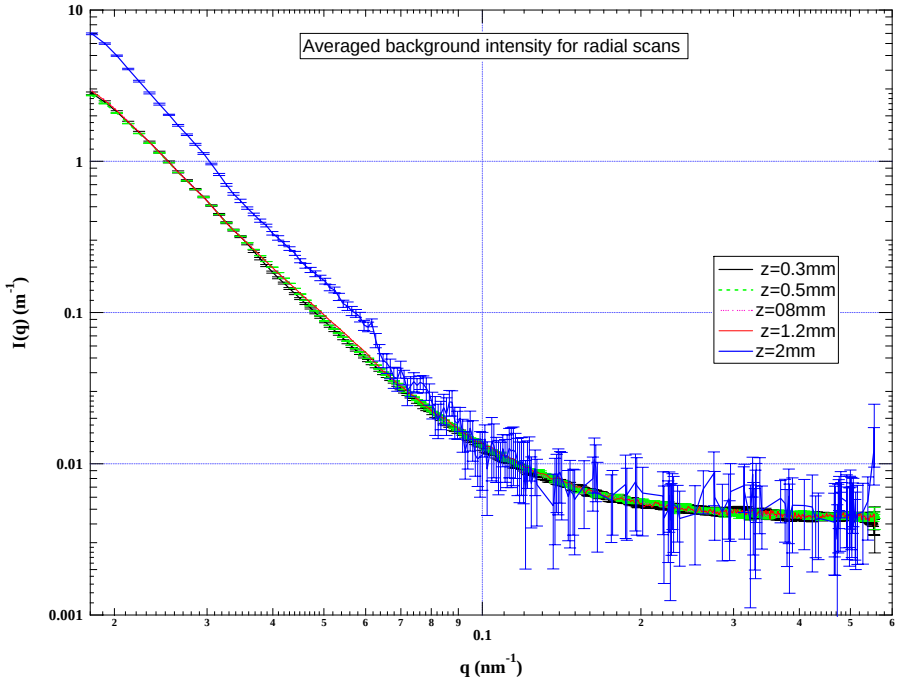

Figure 3 *Example of averaged background scattering intensities for radials scans(n=5) at different axial positions, error bar width ±1σ*

The measurements in the jet show a clear distinction in the scattering profile as a function of the radial and axial position. Due to the improved setup, we were able to conduct measurements on the jet, which were stable in time compared to the previous campaign (ME-864) [4]. Figure 4 shows some exemplary measurements for CO_2 and Phytosterol. The measurements per scan are fairly reproducible and allow for a clear distinction of the measurement position for a radial distance from the centerline up to 1mm. For most scans, at least 5 measurements per position were performed to gain statistical data.

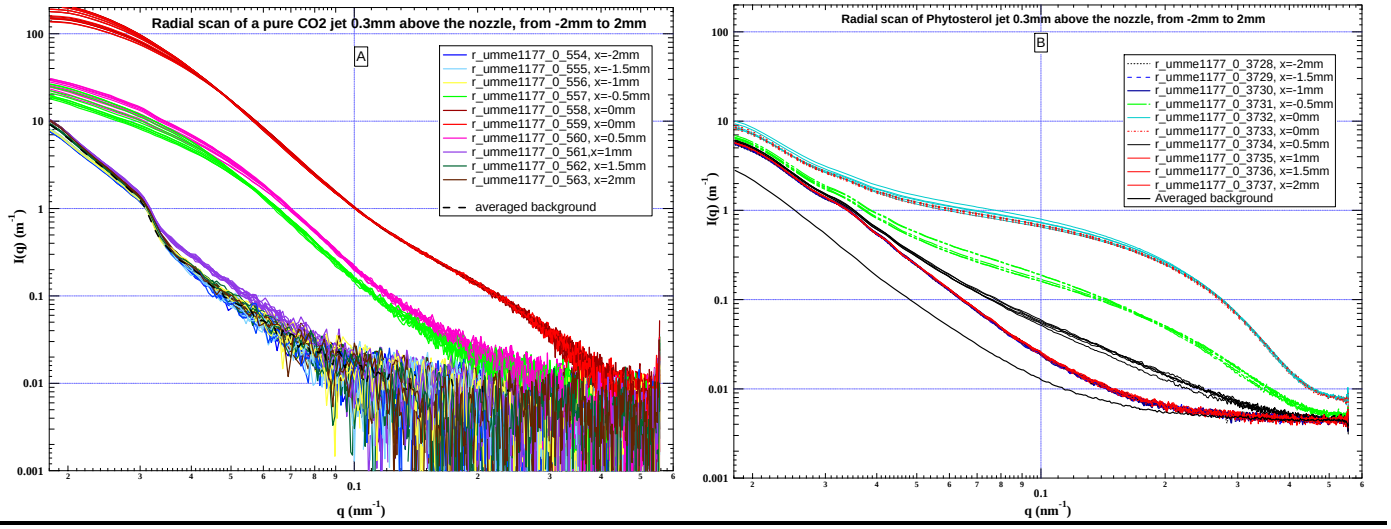

Figure 4 *Horizontal scan of a pure CO_2 (A) and a CO_2 Phytosterol jet (B) 0.3mm above the nozzle*

Figure 4 shows a contour plot of a pure CO_2 jet (no solute) with droplet radii obtained from the scattering curves by applying the unified fit function [4] to the available scattering data between 0.02 and 0.6nm^{-1}. The actual radius is related to the obtained radius of gyration R_g by R=1.3 R_g assuming spherical geometry. It is visible how CO_2 droplets grow rapidly by condensation after the Mach Disk (discontinuity in pressure), which is approximately located at 0.5mm, and evaporate again after reaching a maximum size approximately 1-1.3mm after the nozzle exit. The quality of the fit was satisfying, as can be seen from Figure 5, where the radial scattering curves at two different axial levels, together with the fit, are shown. A reliable fit beyond 1mm radial distance from the centerline of the jet can not be made, since the intensity curve is very noisy after subtracting the background signal, or is even not distinguishable from the latter. It should be mentioned that the interpretation of the results rely solely on the q-range accessible with the pinhole setup

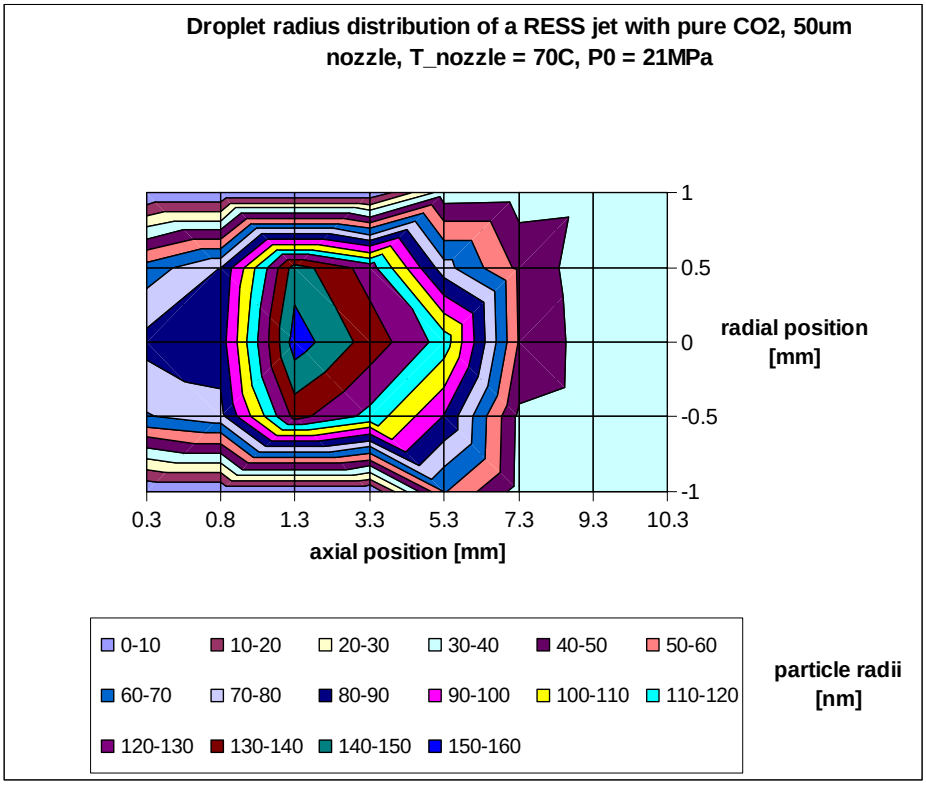

Figure 5 *Particle radius distribution of a RESS jet with pure CO_2*

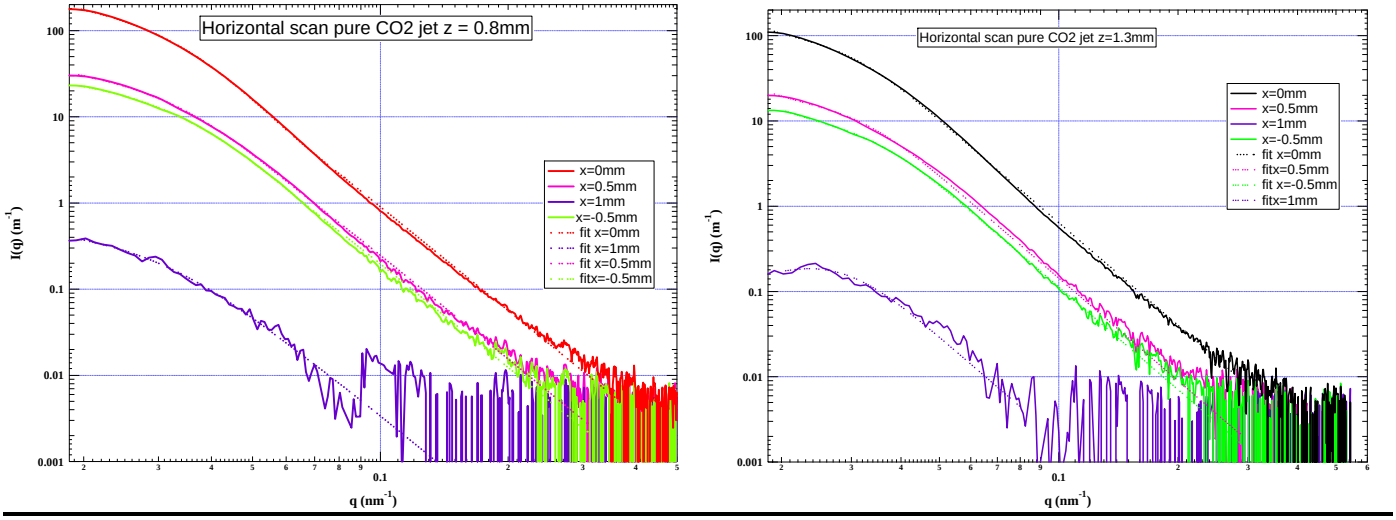

Figure 6 *Background corrected and averaged intensity scattering curves for a pure CO_2 jet at two different axial positions. The dotted lines represent the unified fit function for spherical particles*

For the measurement with particles in the jet however, the approach using the unified fit function did not yield satisfying results yet. Figure 6 shows an attempt of a fit for Phytosterol. The fit deviates in the high q (>0.3nm^{-1}) region significantly from the Porod law (~q^{-4}), especially in the central part of the jet where high gas and particle concentrations are to be expected. The outer regions of the jet show again a satisfying fit. The evaluation process is ongoing at this moment.

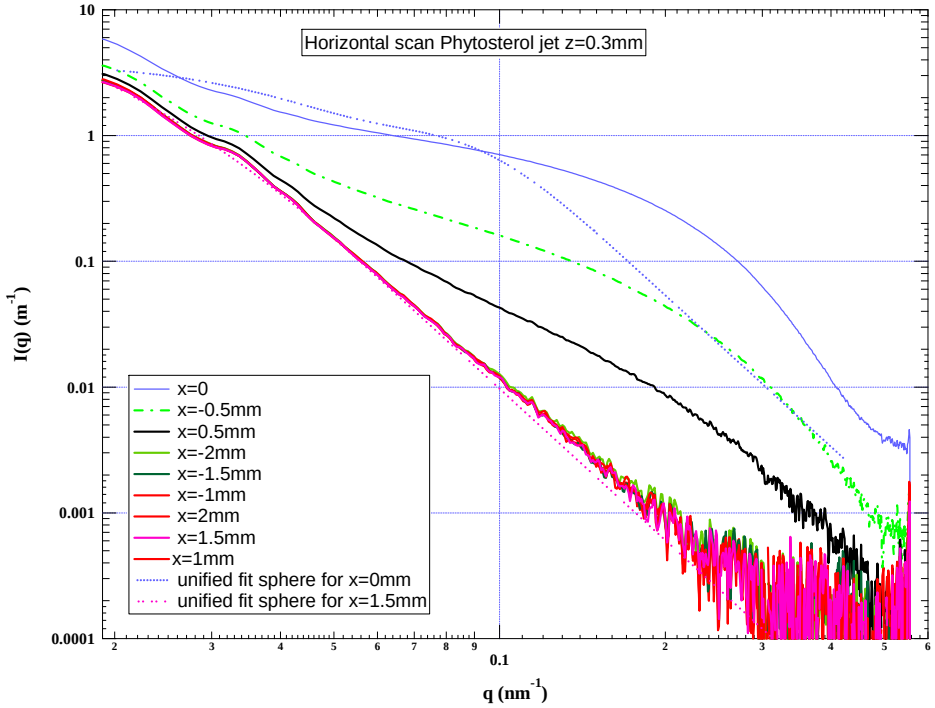

Figure 7 Background corrected and averaged intensity scattering curves at axial position x=0.3mm for a jet with Phytosterol

Summary

The measurement time granted to our team allowed us for the first time to scan the RESS jet, enabling us to resolve the particle size distribution in the jet. These data are needed to improve the modelling of the jet and hence the possibility of process optimisation with regard to particle size and distribution. Particle sizes can be resolved in this dilute system as a function of radial and axial position. Data for a pure CO_2 jet indicate droplet radii from approx. 30 to 155nm in the first 10mm of the jet with a size maximum at about 1.3mm

The jet was mostly stable in time. However, the measured scattering intensity varied from one substance to the other, and showing as well lower signal intensity for a jet with particles compared to a pure CO_2 jet, taking into account similar or even higher beam fluxes and similar attenuator settings for the experiments with particles. This may lead to the conclusion, that the condensation process of CO_2 during the rapid expansion can not be regarded independent from the particle nucleation, as it was assumed in the theoretical description of the RESS process so far [3]. The intention to subtract the scattering intensities from a pure CO_2 jet from those of a RESS jet with particels has to be reconsidered.

Further data analysis will include the evaluation of polydispersity. The results of a complete data evaluation of all substances will be submitted for publication once the evaluation process is finished. However, the available q-range from 0.02nm^{-1} to 0.6nm^{-1} does not cover the bigger aggregates and particles, which are being generated in the jet. Hence, the information obtained from this q-range about particle size and shape distribution in the jet is lacking data about formation of higher aggregates. USAXS measurements would extend the view as well on aggregates and their fractal dimension and hence complete the picture on the nucleation and aggregation process.

Acknowledgment
We would like to thank especially Dr. Pierre Panine from ESRF for his competetent support and guidance on the operation of the SAXS beamline, as well as Dipl.-Inf. Nadine Fritz (ESA), Michael Steurenthaler and Matthias Kern (ITTK) for their good collaboration during the long hours at the beamline.

References

[1] Tom, J. W., Debenedetti, P. G.; Particle Formation with Supercritical Fluids - A Review; *J. Aerosol Sci*. **22** (1991), 555-584
[2] Türk, M., Formation of small organic particles by RESS: Experimental and Theoretical Investigations, *J. Supercrit. Fluids* **15** (1999): 79-89
[3] Helfgen B., Türk M., Schaber K.: Hydrodynamic and Aerosol Modelling of the Rapid Expansion of Supercritical Solutions (RESS-Process); *J. Supercrit.Fluids*, **26, 3**, (2003) 225-242.
[4] Lindner, R.; Türk, M.; Experiment Report ME-864, http://ftp.esrf.fr/pub/UserReports/29662_A.pdf
[5] Beaucage, G., Kammler, H., Pratsinis, S., Particle size distributions from small angle scattering using global scattering functions *J. Appl. Cryst.* (2004) **37**, 523-535